Journal of Power Sources 195 (2010) 5252–5257

Contents lists available at ScienceDirect

Journal of Power Sources

journal homepage: www.elsevier.com/locate/jpowsour

Stability and performance improvement of a polymer electrolyte membrane fuel cell stack by laser perforation of gas diffusion layers

Dietmar Gerteisen*, Christian Sadeler

Fraunhofer Institute for Solar Energy Systems ISE, Department of Energy Technology, Heidenhofstrasse 2, 79110 Freiburg, Germany

ARTICLE INFO

Article history:
Received 23 November 2009
Received in revised form 5 February 2010
Accepted 8 March 2010
Available online 15 March 2010

Keywords:
Proton exchange membrane fuel cell
PEFC stack
Liquid water transport
Flooding
Laser perforation
Gas diffusion layer

ABSTRACT

The performance and stability of a hydrogen-driven polymer electrolyte membrane fuel cell stack (6-cell PEFC stack) are investigated with regard to pore flooding within the gas diffusion layers (GDLs). Two short stacks with various GDLs (Toray TGP-H-060 untreated and laser-perforated) were characterized at different operating conditions by several characterization techniques such as constant current load, polarization curve, chronoamperometry and chronovoltammetry. The experimental results reveal that the perforation of the cathode GDLs improves the water transport in the porous media and thus the performance as well as the stability of the operating stack in medium and high current density range. A reduced pore flooding is verified when using the customized laser-perforated GDLs. The GDL perforation has a huge potential to balance the inhomogeneous in-plane saturation conditions between the inlet and outlet area of the cell and to compensate to a certain degree the effects of temperature distribution within a stack regarding the water management.

1. Introduction

The gas diffusion layer (GDL) in a fuel cell is a specially engineered porous media that combines a variety of basic tasks of fluidic, electric and thermal management [1]. As the name implies the GDL is responsible for a homogeneous distribution of the reactants by diffusion from the gas channel placed in the bipolar plate to the active catalyst layer. It is also needed for the removal of the reaction heat and the products which can be in gaseous or liquid phase depending on the operating conditions. Additionally, the GDL provides the pathway for the electrons and gives the membrane electrode assembly (MEA), sandwiched between two GDLs, mechanical stability. To fulfill all these different tasks the GDL material has to be thermal and electric conductive with a complex porous micro-structure.

In general, three main types of carbon fiber substrates are employed as gas diffusion layer in polymer electrolyte membrane fuel cells (PEFCs): carbon paper, carbon cloth and carbon nonwoven [2]. The carbon fibers are relative good conductors but are not sufficiently hydrophobic to prevent pore flooding at wet conditions [3]. Thus, GDLs are generally treated with a hydrophobic agent such as PTFE to improve the water expel out of the structure. Literature data show that the optimal PTFE content spreads between 10% and 30% with regard to the operating conditions [4–7]. A too high hydrophobic characteristic of the GDL prevents water storage in the void space and thus can lead to membrane dehydration. The sensible characteristics of the wetting properties show that the GDL plays a pivotal role in the water management with still large optimization potential. Due to the geometric constraints of the flow field there are locally inevitable inhomogeneous conditions in the fluid and heat transport that require different requests for the GDL properties under the land and channel area.

In the work of Gerteisen et al. [8] the positive impact of a systematic GDL perforation on the performance of a small test fuel cell with an active area of 1 cm^2 is reported. The laser-cut holes with a diameter of approximately 80 μm are spaced along the channel at a distance of 1 mm. A comparison with a standard, non-modified GDL shows that the performance with the perforated GDL suffers less from accumulated liquid water. The cathode overpotential shows less limitation of the oxygen transport. An increase in the limiting current density of 8–22% with the perforated GDL has been achieved. A comparison of chronoamperometry data shows clearly reduced overshoot behavior, ending in a higher current density value in case of the perforated GDL. This highlights the achievement of less pore flooding and an enhanced water transport in the GDL. These results show that the potential to optimize the GDL structure with regard to liquid water transport, resulting in a reduced water accumulation and minimized oxygen diffusion limitation, is still very large.

* corresponding author. Tel.: +49 761 4588 5205; fax: +49 761 4588 9000.
E-mail address: dietmar.gerteisen@ise.fraunhofer.de (D. Gerteisen).
URL: http://www.ise.fraunhofer.de (D. Gerteisen).

0378-7753/$ – see front matter © 2010 Elsevier B.V. All rights reserved.
doi:10.1016/j.jpowsour.2010.03.021

Table 1
Through-plane and in-plane permeabilities of gas diffusion layers determined by Lattice-Bolzmann flow simulations [10] and measurements [9].

Permeability	In-plane		Through-plane	
	Simulated	Measured	Simulated	Measured
Toray TGP-H090	$11.5 \cdot 10^{-12}$ m^2	$15 \cdot 10^{-12}$ m^2	$7.4 \cdot 10^{-12}$ m^2	$8.99 \cdot 10^{-12}$ m^2
SGL10BA	$30.9 \cdot 10^{-12}$ m^2	$60 \cdot 10^{-12}$ m^2	$21.1 \cdot 10^{-12}$ m^2	$37.4 \cdot 10^{-12}$ m^2

For improving the liquid water removal out of the GDL, two physical properties of the GDL indicate the good potential of the perforation technique:

- Experimental data of Gostick et al. [9] proved by simulation results of Schulz et al. [10] show that the in-plane permeability of liquid water in the GDL is up to twice as much than the through-plane permeability due to the preferred orientation of the carbon fibers (Table 1).
- The smaller the pore radius r_p of a hydrophobic porous structure (contact angle $\theta > 90°$), the higher is the essential water pressure p_{H_2O} to fill these pores (according to the capillary pressure p_c defined by Young–Laplace equation $p_{H_2O} - p_{air} > p_c = r_p^{-1} 2\sigma \cos[\theta]$).

Therefore, providing well-orientated water transport channels (WTCs) in the GDL structure that have larger radii than the mean pore size distribution can improve the liquid water transport from the catalyst layer towards the flow field.

Fig. 1 shows schematically the concept of the water transport enhancement by GDL perforation. Water is generated by the ORR in the CCL and dragged by the protons from the anode side. The water accumulates in the porous structure of the CL, resulting in an increasing liquid water pressure. The existing pressure gradient forces the water out of the CL into the GDL. Here, the water follows the path with the lowest resistance, which is the path with the highest permeability, the in-plane direction. Several water pathways in smaller pores combine to one pathway in a larger pore in order to reduce the water pressure. At the end the water finds a way out of the GDL but with a high tortuosity. Additionally, the rib structure of the flow field, that generally covers about the half of the GDL area, impedes the direct water removal since some pathways lead to dead-end, clogging the GDL in this region.

By means of the laser perforation technique, WTCs with a desired radius can be generated on favored local positions. Due to the high in-plane permeability, the WTCs act as water collecting points from the surroundings. The water fills the WTCs and is forced to move towards the flow field where it evaporates or get carried away by the air stream. Therefore the water saturation in the natural structure of the GDL is reduced, leading to an improved oxygen access to the CL.

The performance improvement in the single cell experiments due to a better water removal of the modified GDL motivates the transfer of the laser perforation technique from a single cell to a industrial relevant stack for portable applications. An already existing 6-cell stack (see Fig. 2) was chosen for characterizing the influence of GDL perforation concerning flooding phenomena.

2. Experimental and discussion

2.1. Preparation of the GDL

A standard Toray paper (TGP-H-060, thickness 190 μm) is modified by producing large pores (water transport channels, WTCs) with a tortuosity of one for the capillary diffusion of liquid water, so that the water can diffuse without requiring large pressure gradients. A detailed description of the GDL perforation by a laser beam and the advantage of this technique is given in [8].

2.1.1. Fuel cell stack and operating conditions

The stack consists of graphite compound bipolar plates with an active area of 30.87 cm^2 per cell, in which on both sides,

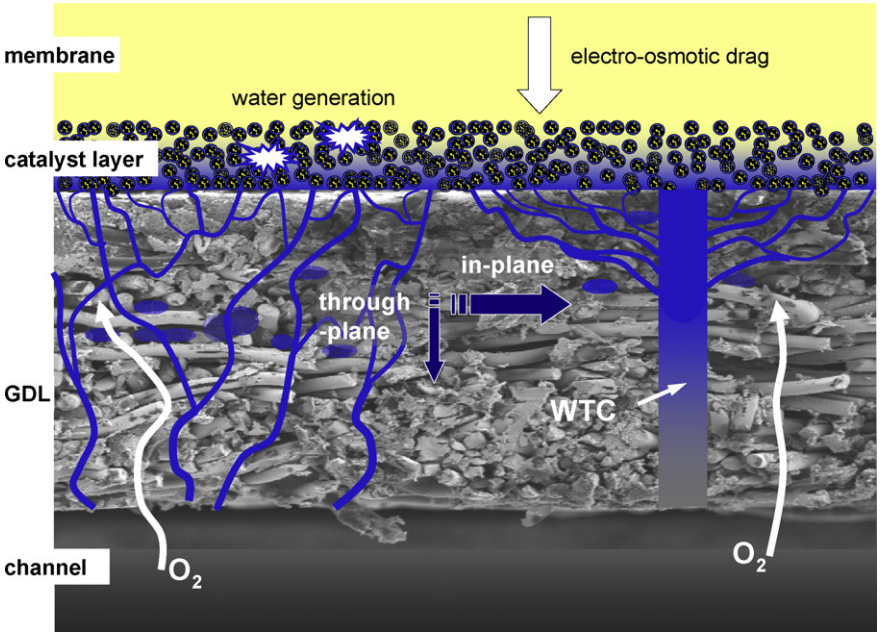

Fig. 1. Schematic of the liquid water transport with and without water transport channel.

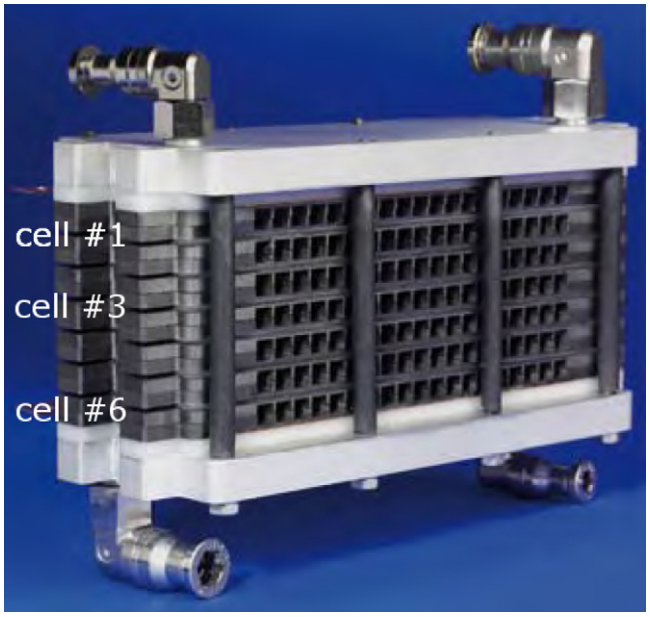

Fig. 2. A 6-cell stack was used to investigate the effects of GDL perforation on the performance.

cathode and anode, a double-channel serpentine flow field is machined to deliver the reactants across the active area homogeneously. Similar to the single cell experiments [8], MEAs from Gore™ (PRIMEA® Series 5510, loading$_{c/a}$: 0.4/0.4 mg cm^{-2}, thickness: 35 μm) were assembled. This time, GDLs of type Toray TGP-H060 with a thickness of 190 μm (instead of 280 μm, used in the single cell experiments) were investigated since this kind of GDL is originally attached and well characterized for this stack.

Again, only the cathode GDLs were modified by laser treatment. WTCs with the same diameter of approximately 80 μm are placed beneath the channel along the serpentine flow field with a pitch of 1 mm, leading to approximately 950 holes over the entire GDL area. Fig. 3 shows a drawing of the flow field with the position of the WTCs.

The stack temperature is regulated with a controllable fan, blowing through cooling channels that are visible in Fig. 2. Such an air cooling system is not able to achieve a homogeneous temperature distribution throughout the stack.

The outer cells (cell #1 and #6) are mostly cooler than the inner cells due to the additional heat dissipation via the end plates and the fact that only one adjacent cell acts as heat source. A further drawback of air cooling compared to water cooling (like in the single cell experiments) is the limited cooling capacity that complicates the temperature control. Thus, in the following experiments either a constant cooling capacity by a constant fan power was adjusted, leading to relatively high temperature differences for high and low load, or the temperature was controlled, leading to some temperature oscillations of ±1 ° C caused by the control. The stack temperature was measured by thermo couples on the surface of the bipolar plate in the middle of the stack. On the anode side, the stack was operated in "open end" mode (no recirculation of unutilized hydrogen).

A potentiostat from Zentro (EL 3000/60/ 125) with a maximum current capability of 125 A and a voltage range up to 60 V was used for the experiments. A single cell voltage tap is embedded on the stack to assign the monitored flooding event to the specific cells in the stack. A more detailed description of the stack, its performance and the test bench is given in Shimpalee et al. [11].

Several characterization techniques on different operating conditions were applied to investigate the influence of the GDL perforation on the water management:

- *Constant current load*. The cell was operated in galvanostatic mode at a constant current of 22 A (approximately 0.65 A cm^{-2}) that corresponds to a single cell voltage in the range of 0.5–0.6 V which is the optimal operating point concerning the interplay of power density, efficiency and stability for this stack in a system. In this mode a stable operation is desired with less purge events.[1] The mass flow controls of air and hydrogen were adjusted to a stoichiometry (λ) of 2.5 on the cathode side and 1.5 on the anode side. Both gases were humidified to a dew point of 35 ° C (as in all further stack experiments). The stack temperature was controlled to 63 ° C by two fans.
- *Polarization curve*. Starting from OCV, the load was increased stepwise by 2 A until the single cell voltages reached a value of about 0.4 V. Then the experiment was stopped to prevent irreversible degradation since the voltages became unstable. Every current point was maintained for 5 min. A stoichiometry of $\lambda_{air} = 2.5$ and $\lambda_{H_2} = 1.5$ was chosen. At the beginning of each current step a purge event was initiated. The stack temperature was controlled to 63 ° C by the fan.
- *Chronoamperometry*. The stack voltage was stepped between 4.8 V and 3.6 V. To ensure repeatability 10 cycles were performed, whereby every voltage level was maintained for 200 s. The mass flow rates were set to $\dot{V}_{air} = 4.3\,\mathrm{l\,min^{-1}}$ and $\dot{V}_{H_2} = 1\,\mathrm{l\,min^{-1}}$. Since the temperature control is not able to fix a constant temperature for such high dynamic load changes, a continuous cooling power was adjusted by setting a constant fan voltage. Hence, the stack temperature increased with increasing current density due to increased reaction and ohmic heat. The higher temperature has a promotive effect to prevent flooding events since the saturation pressure increases with temperature that makes a direct comparison of two relaxation curves with different temperatures difficult.
- *Chronovoltammetry*. The stack current was stepped between 10 A and 15 A. 10 cycles were applied, whereby every current level was maintained for 200 s. Again, mass flow rates of $\dot{V}_{air} = 4.3\,\mathrm{l\,min^{-1}}$ and $\dot{V}_{H_2} = 1\,\mathrm{l\,min^{-1}}$ were adjusted and the same constant fan voltage for cooling as for the chronoamperometry was chosen.

Since the increased reaction and ohmic heat at higher current density causes a higher stack temperature which in turn results in an improved oxygen reduction reaction, higher evaporation rates and a better oxygen diffusivity due to a lowered saturation of the porous media, an amplifying effect between temperature and current increase is activated that makes the separation of the influence of the GDL perforation and temperature effects difficult. By applying chronovoltammetry, the same current density steps are given for both stacks and hence more or less the same heat sources. Therefore, the temperature of Stack$_{perf}$ should be at least the same as Stack$_{org}$ or even lower if the fuel cell losses are decreased by GDL perforation and thus the amplifying temperature effect of performance / heating does no longer exist with this measurement technique.

2.2. Characterization of a modified GDL in a fuel cell stack

2.2.1. Constant current load

As mentioned before the air cooling system is not able to achieve a homogeneous temperature distribution throughout the stack. The

[1] Purge event: the gas flow rates were automatically increased to $\dot{V}_{air} = 15\,\mathrm{l\,min^{-1}}$ and $\dot{V}_{H_2} = 3.5\,\mathrm{l\,min^{-1}}$ for a period of 5 s by the stack control to carry out water if a maximum voltage difference of 120 mV between the cells was exceeded.

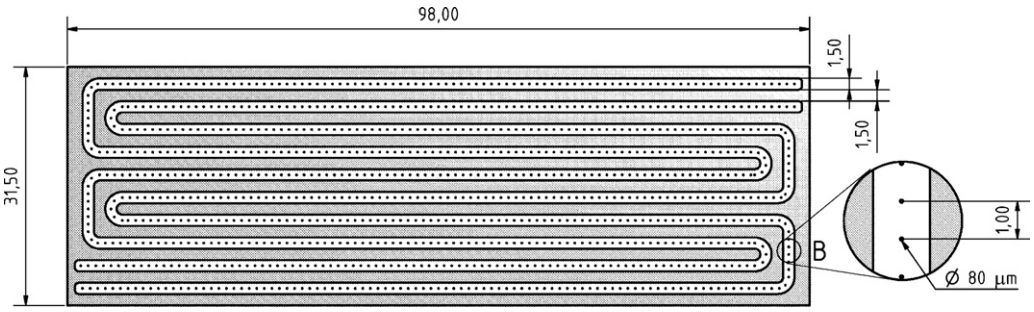

Fig. 3. Schematic drawing of the position and size of the holes along the flow field.

existing temperature gradient from the cooler outer cells to the warmer cells inside the stack leads to inhomogeneous humidification conditions since the saturation, correlated with the relative humidity of the air, is a strong function of the temperature. Thus, a temperature variation of few degrees Celcius along the stack can lead to supersaturation of the gases in the outer cells whereby the water pressure is still below the saturation pressure in the inner cells. In the outer cells further evaporation of the generated water is suppressed and condensation of vapor starts leading to liquid water accumulation in the porous media and in the flow field structure. Thus, the outer cells tend to flood rather than the inner cells. Therefore it is expected that the GDL perforation has a huge advantage especially for the outer cells.

Fig. 4 shows the cell voltages of an outer cell (cell #1) and an inner cell (cell #3) at a constant current of 22 A for a period of nearly 30 min for a stack with modified and non-modified GDL. For the sake of clarity not all single cell voltages are shown, but it can be stated that cell #3 is representative for all inner cells and that the characteristic of cell #1 is similar to cell #6. In the following only these two representative voltages are analyzed to determine the influence of the two temperature extremes within these cells. Additionally, the measured stack temperature is plotted.

First of all, it can be seen that the cells within the stack with perforated cathodic GDLs ($Stack_{perf}$) show higher voltages than the cell within the stack with the original GDLs ($Stack_{org}$). The voltage of the inner cell of the $Stack_{perf}$ shows a stable value of about 0.575 V, compared to 0.53 V of the inner cells of $Stack_{org}$. Critical are the unstable voltages of the outer cells of both stacks, but again $Stack_{perf}$ shows the higher value. It can be clearly seen that the voltages of the outer cells are responsible for the activation of the air flow pulse by the stack control to prevent a dramatical collapse of the cell voltage. During the shown time of about 30 min four air flow pulses were required to prevent dramatical performance breaks for $Stack_{org}$, whereas only one pulse after 1400 s was sufficient for $Stack_{perf}$. This shows that $Stack_{perf}$ suffers less on accumulated liquid water.

The temperatures of both measurements were controlled to 63 °C, whereby an alternating temperature of about ±0.5 ° C could not be avoided by the temperature control. This small temperature deviation couples with the cell voltages, especially of the voltage of the outer cells, that highlights a high sensitivity of the water management with the temperature in this operating point.

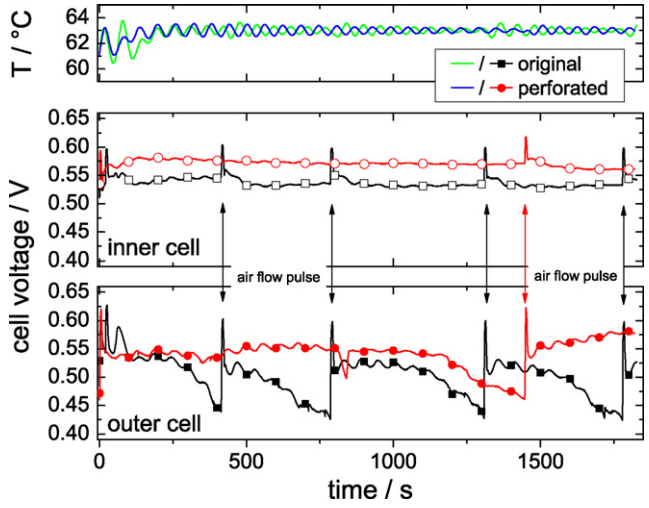

Fig. 4. Stability test of both stacks at a constant load of 22 A shows a higher voltage level and less cell voltage breaks in case of perforated GDLs than with the original ones.

2.2.2. Polarization curve

Voltage–current curves of the problematic cell #1 within $Stack_{org}$ and $Stack_{perf}$ are shown in Fig. 5. The stack was operated in galvanostatic mode. The black/red marks in the polarization curves are all the measured voltage data within the 5 min current step.

Two features are evidently, on the one hand the cell voltage of $Stack_{perf}$ decreases slower with increasing current density than that of $Stack_{org}$ which results in a higher current density. On the other hand the variance of the cell voltages of $Stack_{org}$ is much higher than for $Stack_{perf}$ indicating an improved water management of $Stack_{perf}$. It is noticeable that the voltage at 0.65 A cm^{-2} is most stable for both stacks. The reason is the temperature control by air cooling that is less stable for low current densities where the heat generation is small. Up to a current density of 0.65 A cm^{-2} the control causes temperature variations of 2 ° C that results in small voltage variations (approximately 5 mV). The small temperature variation seems to encourage flooding also in the low

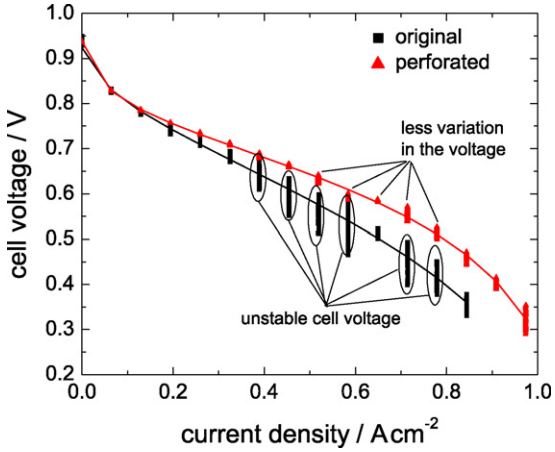

Fig. 5. A comparison of polarization curves of cell #1 between $Stack_{org}$ and $Stack_{perf}$.

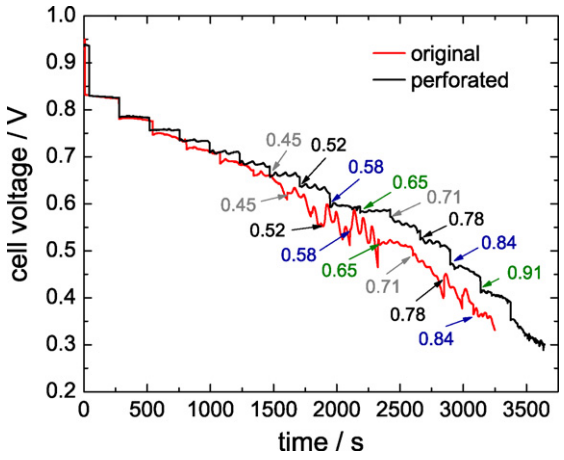

Fig. 6. The voltage of cell #1 versus time is visualized for both stacks.

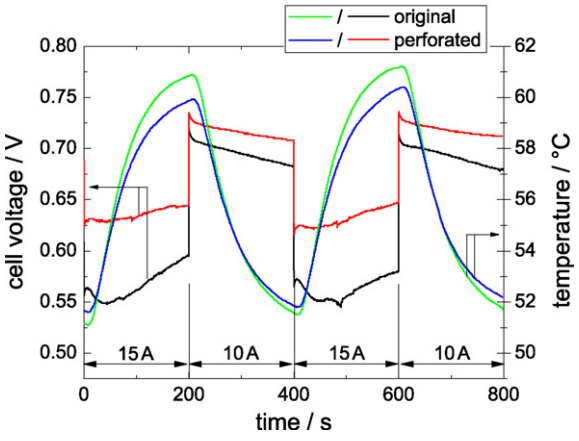

Fig. 8. Chronovoltammetry measurements show a better performance of $Stack_{perf}$ despite of a lower stack temperature.

current density region that is more pronounced in the measurements of $Stack_{org}$. At a current density of 0.65 A cm^{-2} and above, the temperature control is more stable, which is visible in slightly smaller voltage variations. With a further increase in current density $Stack_{org}$ tends more and more to flood, measured in the voltage decrease.

The same data as used for Fig. 5 are plotted as voltage-time curve in Fig. 6, where some current steps are marked by arrows (in A cm^{-2}). The plot shows clearly the periodic instable operation of $Stack_{org}$, beginning at a current density of 0.45 A cm^{-2}. Voltage plateaus for the different current steps are not visible anymore. The voltage of $Stack_{perf}$ is nearly stable up to 0.91 A cm^{-2} with only a slight decrease over time. This experiments show that the GDL perforation improves the stack performance and stability.

2.2.3. Chronoamperometry

The current relaxation on a voltage step is investigated for both stacks in Fig. 7.

The stack voltage was switched between 4.8 V and 3.6 V that corresponds to an average voltage step per single cell of 800 mV and 600 mV, comparable to the single cell experiments. A distinct enhancement of the current density was achieved especially at low voltages. The characteristics of the relaxation curves are similar to the measurements with the small single cell [8]. A small overshoot

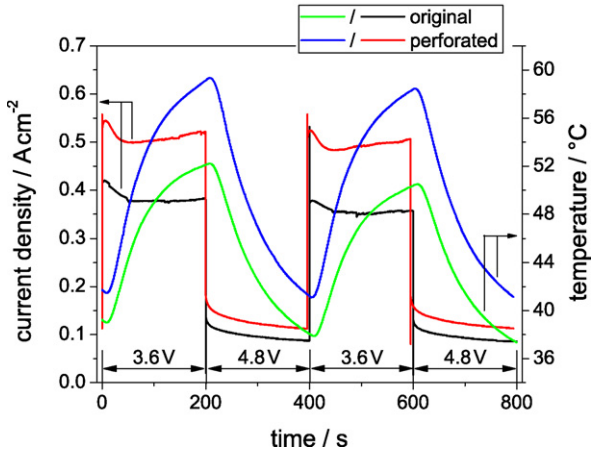

Fig. 7. The current response on voltage step changes between 4.8 V and 3.6 V differ clearly between the stack with untreated and perforated GDLs.

is visible on stepping from 4.8 V to 3.6 V which can be explained by a temporally delayed increase of the saturation related to the current increase, resulting in increasing mass transport limitations. The experiments were made with a constant (non-controlled) air cooling, thus the temperature rises about 11 ° C ($Stack_{org}$) and 18 ° C ($Stack_{perf}$). The higher current density of $Stack_{perf}$ causes higher heat production, resulting in a higher stack temperature. The increased temperature in turn improves the reaction kinetics and reduces the saturation by higher evaporation rates. Thus, the direct comparison has to be treated with respect. Nevertheless, the WTCs have a positive influence on the water management and therefore on the fuel cell stack performance because the operating conditions of both experiments were equal.

2.2.4. Chronovoltammetry

To elude the chicken or the egg causality dilemma of current and temperature, a similar experiment was made in galvanostatic mode where the stack current was switched between 10 A and 15 A. Galvanostatic measurements have the advantage of comparable heat generation because the current determines the ohmic and the reaction heat, which are the main heat sources in fuel cells [12]. In Fig. 8 the cell voltage response on current steps shows a better performance for the $Stack_{perf}$ again. An enhancement of about 50–60 mV in cell voltage was achieved at 15 A. Every fuel cell loss such as ohmic, mass and charge transfer loss causes an increase in the electrode overpotential which in turn increase the heat generation at a certain current density. Thus, an increased mass transport of the reactants leads to a lower temperature at that certain current density. Since a lower temperature provoke higher relative humidity and increased condensation, leading to a higher saturation of the porous media, $Stack_{perf}$ should show a lower performance from that point of view. For this reason, a performance improvement due to a temperature effect can be excluded, since the temperature of $Stack_{perf}$ is lower than $Stack_{org}$ in this experiment. The lower temperature of $Stack_{perf}$ indicates a lower heat generation due to an improved mass transport. Consequently, one can claim that the temperature effect is not the determining influence for the improved performance for both experiments and thus can be attributed to the GDL perforation by improving the water transport from the CL via the GDL to the channel.

2.3. Discussion

The restructuring of a cathode GDL by laser perforation technique was effectually transferred from a small test cell (see [8])

to a fuel cell stack with relevant size for portable applications. The shown experimental results reveal that the GDL perforation improves the performance as well as the stability of an operating stack in the medium and high current density range. A reduced pore flooding is definitely verified when using the customized GDLs. The problems caused by an inhomogeneous temperature distribution throughout the cells within the stack, leading to water management problems for the cooler outer cells, is still visible for both stacks. However, the drastic collapses in performance observed in the outer cells of the unmodified stack could be reduced by the GDL perforation leading to less purge events.

By using perforated cathode GDLs, a lowered saturation of the porous media leads to a reduced water back diffusion to the anode side which in turn can increase the time interval between anode purge events. This improves the hydrogen utilization and thus the system efficiency. The more stable operation with the perforated GDLs leads to a easier stack control.

The restructuring of GDLs within the stack was applied with the same strategy as for the single cell. The WTCs were located beneath the channel structure with the same diameter and pitch. Because the hole arrangement, shape and size has not been optimized yet, hidden potential for the water management improvement is assumed by this technique. In-plane inhomogeneities due to temperature, reactant and vapor concentration could be compensated to a certain degree by, e.g. graduated WTC pitch or size. The resulting problems of the outer cells due to their lower temperature could be minimized by differentiating the perforating strategy between inner and outer cells. Combining structured GDLs with unstructured or structured MPLs together with selective hydrophobizing/philizing of some parts of the GDL show promise of achieving an optimized GDL design.

3. Conclusion

PEM fuel cell stack measurements show an improved liquid water transport from the catalyst layer towards the flow field with laser-perforated cathodic GDLs. Performance as well as transient analysis show lower overpotential and higher stability in the medium and high current density range with perforated GDLs that can be clearly attributed to a minimized pore flooding. The potential to optimize the GDL structure with regard to liquid water transport is still very large since the arrangement of the WTCs and their design has not been optimized yet.

References

[1] R.P. Ramasamy, E.C. Kumbur, M.M. Mench, W. Liu, D. Moore, M. Murthy, International Journal of Hydrogen Energy 2008 (33) (2008) 3351–3367.
[2] C. Quick, D. Ritzinger, W. Lehnert, C. Harting, Journal of Power Sources 190 (1) (2009) 110–120.
[3] C. Ziegler, D. Gerteisen, Journal of Power Sources 188 (1) (2009) 184–191.
[4] G.-G. Park, Y.-J. Sohn, T.-H. Yang, Y.-G. Yoon, W.-Y. Lee, C.-S. Kim, Journal of Power Sources 131 (1–2) (2004) 182–187.
[5] E. Giorgi, L. Antolini, A. Pozio, E. Passalacqua, Electrochimica Acta 43 (24) (1998) 3675–3680.
[6] J. Moreira, A.L. Ocampo, P.J. Sebastian, M.A. Smit, M.D. Salazar, P. del Angel, J.A. Montoya, R. Prez, L. Martnez, International Journal of Hydrogen Energy 28 (6) (2003) 625–627.
[7] C. Lim, C. Wang, Electrochimica Acta 49 (24) (2004) 4149–4156.
[8] D. Gerteisen, T. Heilmann, C. Ziegler, Journal of Power Sources 177 (2008) 348–354.
[9] J. Gostick, M. Fowler, M. Pritzker, M. Ioannidid, L. Behra, Journal of Power Sources 162 (2006) 228–238.
[10] V.P. Schulz, J. Becker, A. Wiegmann, P.P. Mukherjee, C.-Y. Wang, Journal of the Electrochemical Society 154 (4) (2007) B419–B426.
[11] S. Shimpalee, M. Ohashi, J.W. Van Zee, C. Ziegler, C. Stoeckmann, C. Sadeler, C. Hebling, Electrochimica Acta 54 (10) (2009) 2899–2911.
[12] D. Gerteisen, T. Heilmann, C. Ziegler, Journal of Power Sources 187 (2009) 165–181.